JOC Article
pubs.acs.org/joc

4-Substituted 1-Acyloxypyridine-2(1*H*)-thiones: Experimental and Computational Studies of the Substituent Effect on Electronic Absorption Spectra†

Aleksandra Jankowiak and Piotr Kaszynski*

Organic Materials Research Group, Department of Chemistry, Vanderbilt University, Nashville, Tennessee 37235

piotr.kaszynski@vanderbilt.edu

Received July 15, 2009

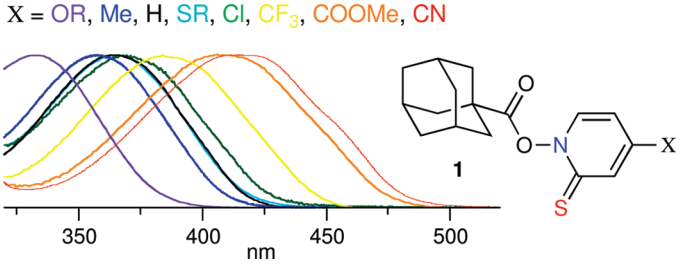

A series of eight 4-substituted 1-(adamantane-1-carbonyloxy)pyridine-2(1*H*)-thiones (**1**, X = H, OC_7H_{15}, Me, CF_3, SC_3H_7, CN, COOMe, and Cl) was prepared and characterized by UV−vis spectroscopy in MeCN and cyclohexane. The observed lowest energy transition, designated as $\pi_{CS} \rightarrow \pi^*_{ring}$, exhibits a substantial substituent effect and λ_{max} ranges from 333 (X = OC_7H_{15}) to 415 nm (X = CN). Experimental λ_{max} values for all esters except for **1b** (X = OC_7H_{15}) correlate with the σ_p^- parameter (ρ = 0.41 ± 0.03, r^2 = 0.95). In contrast, the energy of the absorption band at about 295 nm, designated as $\pi_{CS} \rightarrow \pi^*_{CS}$, is practically substituent independent. Both absorption bands exhibit a modest negative solvatochromic effect. The experimental absorption energies correlate better with excitation energies calculated for *N*-acetyloxy analogues **2** with the ZINDO//DFT than with the TD-DFT//DFT method. Calculations for a series of 12 *N*-acetates **2** predict the most blue-shifted $\pi \rightarrow \pi^*$ transition for the alkoxy substituent and most red-shifted for the NO_2 group relative to the parent **2a** (X = H).

Introduction

O-Acyl derivatives of 1-hydroxypyridine-2(1*H*)-thione, so-called Barton esters, are popular precursors of free radicals and are often used as reagents in free radical transformations of carboxylic acids.[1] One such an example is adamantane-1-carbonyloxy derivative **1a**.[1] To date, ring-substituted Barton esters are practically unknown[2,3] despite the fact that a handful of substituted 1-hydroxypyridine-2(1*H*)-thiones, including 4-propyl,[4] 4-fluoroalkyl,[5] mercapto,[6] 4-methoxycarbonyl,[7] 3-ethoxy,[8] and several methyl[8−10] and dimethyl[9] derivatives, have been described in the literature. The substituent

† Presented in part at 9th Annual Florida Heterocyclic and Synthetic Conference (Flohet-9), Gainesville, FL, March 9−12, 2008, and the 237th ACS National Meeting, March 22−26, 2009, Salt Lake City, Utah.

(1) Knight, D. W. In *Encyclopedia of Reagents for Organic Synthesis*; Paquette, L. A., Ed.; Wiley&Sons: New York, 1995; Vol. 4, pp 2775−2778. Crich, D. In *Comprehensive Organic Synthesis*; Trost, B. M., Fleming, I., Ley, S. V., Eds.; Pergamon: New York, 1991; Vol. 7, pp 717−734 and references cited therein.

(2) Edrissi, M.; Jadbabaee, M. J.; Dalziel, J. A. W. *Microchem. J.* **1971**, *16*, 536–537.

(3) Pyridine-2(1*H*)-thiones substituted with methyl (positions 4 and 5) and NO_2 (position 5) were implied in a synthetic scheme, but no details or characterization data were reported: Rao, U. N.; Biehl, E. *J. Org. Chem.* **2002**, *67*, 3409–3411.

(4) Rees, C. W. *J. Chem. Soc.* **1956**, 3684–3685.

(5) Sun, J.-Y.; Qiu, X.-L.; Meng, W.-D.; Qing, F.-L. *Tetrahedron* **2006**, *62*, 8702–8706.

(6) Puszko, A.; Talik, Z. *Pol. J. Chem.* **1991**, *65*, 377–380.

(7) Yale, H. L.; Losee, K.; Martins, J.; Holsing, M.; Perry, F. M.; Bernstein, J. *J. Am. Chem. Soc.* **1953**, *75*, 1933–1942.

(8) Shaw, E.; Bernstein, J.; Losee, K.; Lott, W. A. *J. Am. Chem. Soc.* **1950**, *72*, 4362–4364.

(9) Abramovitch, R. A.; Knaus, E. E. *J. Heterocycl. Chem.* **1975**, *12*, 683–690.

(10) Puszko, A. *Pol. J. Chem.* **1994**, *68*, 657–664.

DOI: 10.1021/jo901522r Published on Web 09/09/2009

SCHEME 1

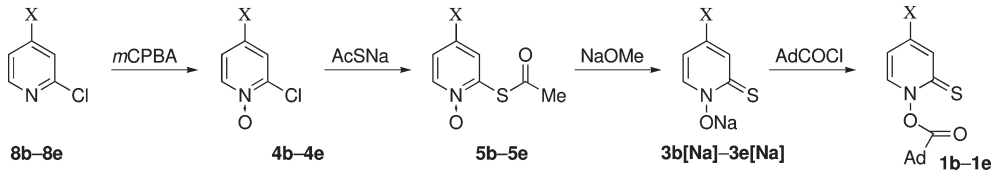

could presumably allow for controlling the sensitivity of the Barton esters to visible light and tune the wavelength of radical chain initiation.[11,12] In addition, appropriately functionalized Barton esters could be incorporated into more complex molecular architectures of radiation/light sensitive functional materials.

In this context, we recently described a method for the preparation of 4-alkoxy-1-hydroxypyridine-2(1*H*)-thiones including **1b**.[13] In contrast to the yellowish parent **1a**, the 4-heptyloxy derivative **1b** is a colorless solid.[13] This finding prompted us to investigate the substituent effect on photophysical properties of Barton esters, and to develop synthetic access to several diverse 4-substituted 1-hydroxypyridine-2(1*H*)-thiones. Here, we describe the preparation and spectroscopic studies of eight esters **1a**−**h** which contain the adamantyl group chosen for the convenience of isolation and purification of the products. For a better understanding of the substituent−photophysical properties relationship in esters **1**, we conducted TD-DFT and ZINDO calculations for a dozen of their acetyl analogues, esters **2**.

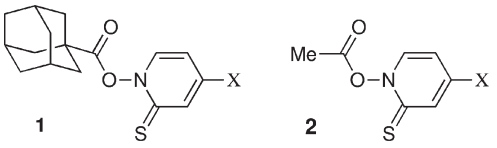

a: X = H
b: X = OC_7H_{15}-*n*
c: X = Me
d: X = CF_3
e: X = SC_3H_7-*n*
f: X = CN
g: X = COOMe
h: X = Cl
i: X = OMe
j: X = SMe
k: X = NMe_2
l: X = OAc
m: X = C≡CH
n: X = NO_2

Results

Synthesis. Adamantane-1-carboxylic acid *O*-esters **1** were prepared by acylation of the corresponding 1-hydroxypyridine-2(1*H*)-thione sodium salts **3**[**Na**] with adamantane-1-carbonyl chloride (Scheme 1). The 4-cyano and 4-chloro derivatives **1f** and **1h** were obtained in a reaction of the acid chloride with appropriate thione **3f** or **3h** in the presence of pyridine. Attempts to generate the sodium salt **3f**[**Na**] from **3f** with use of NaH led to significant decomposition of the substrate. Salts **3b**[**Na**]−**3e**[**Na**] were obtained from 2-chloropyridine *N*-oxides **4b**−**e** according to our recently reported general procedure (Scheme 1).[13] Thus, treatment of **4** with sodium thioacetate gave crude thioacethoxy derivatives **5** which, isolated after acidic workup, were contaminated with the corresponding thiones **3**. Both thioacetates **5** and thiones **3** were sensitive to silica gel and light. Therefore, without rigorous purification the crude products were reacted with MeONa to generate the sodium salts **3**[**Na**] used for the formation of esters **1**. The overall yield for the three-step procedure was 40−66%.

SCHEME 2

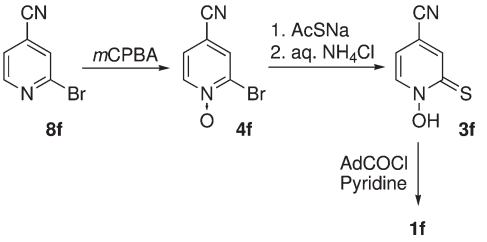

The 4-cyano, 4-methoxycarbonyl, and 4-chloro derivatives exhibited sensitivity to the basic MeONa. Therefore, the 4-cyanopyridine-2(1*H*)-thione (**3f**) was liberated from the thioacetate **5f** by using aqueous NH_4Cl giving an approximately 75% pure product used for the esterification step (Scheme 2). The purity of the thioacetate **5g** obtained either from 2-chloro or 2-bromo *N*-oxide **4g** and AcSNa was low. Therefore, thione **3g** was obtained by using thiourea followed by hydrolysis with aqueous Na_2CO_3, according to a modified patent procedure.[14] Both halides, the 2-chloro and 2-bromo esters **4g**[**Cl**] and **4g**[**Br**], respectively, gave comparable results. The isolated thione **3g** was then converted to the sodium salt **3g**[**Na**] with NaH (Scheme 3) and subsequently to **1g**. Our brief investigation of the formation of the isopropyl analogue of **3g** from **6** demonstrated that the reaction was much less clean and the product was only ~40% pure, and consequently was not pursued further.

The thioacetate route for the preparation of 4-chloro ester **1h** was unsuccessful. Thioacetate **5h** was easily obtained from the known 2,4-dichloropyridine *N*-oxide[15] (**4h**) as a typical mixture with the partially deprotected thione **3h**. However, the reaction of **5h** with MeONa gave multiple products. Attempts to liberate the thione form the thioacetate **5h** by using aqueous NH_4Cl, in a manner analogous to the preparation of **3f**, were plagued with low mass recovery and the formation of multiple products. Therefore, we focused on the reaction of dichloride **4h** with thioacetamide, which was previously used to prepare 2,4-dimercaptopyridine *N*-oxide.[6] Thus, a reaction of **4h** with limited amounts of thioacetamide (1.3 equiv) in an inert atmosphere with use of literature conditions[6] gave, in one instance, a monomercapto derivative in 63% yield. The regioselectivity of the thiolation reaction was established by alkylation of a sample of the isolated

(11) Hartung, J.; Spehar, K.; Svoboda, I.; Fuess, H.; Arnone, M.; Engels, B. *Eur. J. Org. Chem.* **2005**, 869–881.
(12) Arnone, M.; Engels, B. *J. Phys. Chem. A* **2007**, *111*, 3161–3165.
(13) Jankowiak, A.; Jakowiecki, J.; Kaszynski, P. *Pol. J. Chem.* **2007**, *81*, 1869–1877.
(14) Bernstein, J.; Losee, K. A. U.S. patent 2713049, **1955**.
(15) Abramovitch, R. A.; Deeb, A.; Kishore, D.; Mpango, G. B. W.; Shinkai, I. *Gaz. Chim. Ital.* **1988**, *118*, 167–171.

SCHEME 3

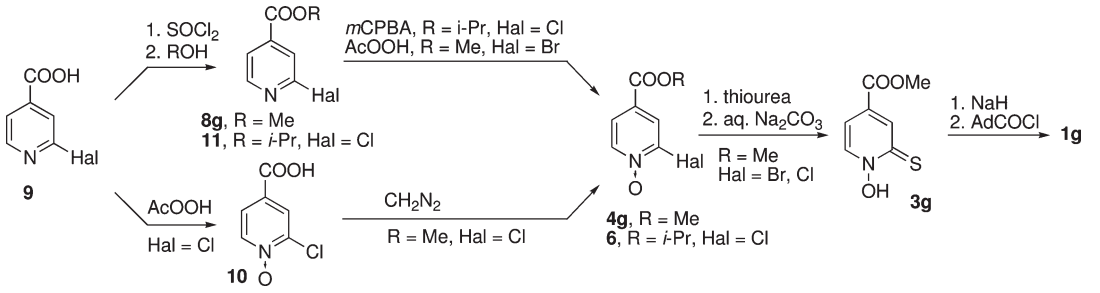

SCHEME 4

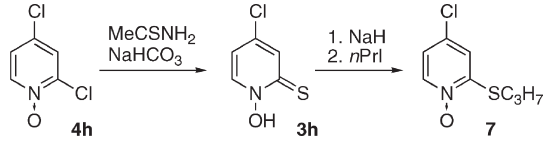

SCHEME 5

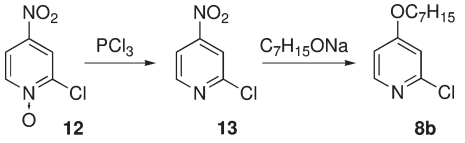

SCHEME 6

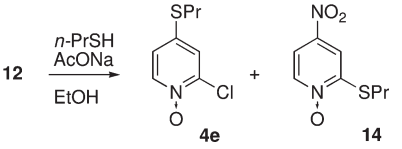

mercaptan with *n*-PrI and comparison of the NMR spectrum for the propylation product **7** with that of **4e** (Scheme 4). The thiolation reaction of **4h** was not reproducible and purification of the thione was often difficult. Consequently, the preparation of ester **1h** was conducted on a crude, about 60% pure, thione **3h**.

All sulfur-containing compounds exhibited sensitivity to white light. Therefore, transformations of oxides **4c**−**h** to the corresponding esters **1** were conducted with careful exclusion of ambient light, and reaction workup and product isolation were performed in the presence of red light. For instance, attempts to prepare thione **3g** from *N*-oxide **4g** in ambient light (fluorescent tube) did not give the expected product; instead a mixture of other products was observed by NMR.

N-Oxides **4b**−**d** and **4f** were prepared by oxidation of the corresponding 2-chloropyridines **8b**−**d** or bromopyridine **8f** with *m*-chloroperbenzoic acid (*m*CPBA, Schemes 1 and 2), while the methyl ester **4g[Br]** was prepared by oxidation of the corresponding ester **8g[Br]** with peracetic acid (Scheme 3). The required ester was obtained from 2-bromoisonicotic acid (**9[Br]**) prepared form 2-amino-4-methylpyridine according to a literature procedure.[16] The chloro ester **4g[Cl]** was obtained by treatment of 2-chloroisonicotinic acid *N*-oxide (**10**) with diazomethane (Scheme 3). The isopropyl ester *N*-oxide **6** was prepared from ester **11** according to a modified patent procedure,[14] using *m*CPBA instead of peracetic acid. The acid **10**[17] was prepared by oxidation of **9[Cl]** with AcOOH (Scheme 3).

The original[13] one-step preparation of 2-chloro-4-heptyloxy *N*-oxide (**4b**) from 2-chloro-4-nitropyridine *N*-oxide (**12**) turned out to be impractical in larger scales. Therefore, we improved the two-step process in which 2-chloro-4-nitropyridine[18] (**13**) was alkoxylated with sodium heptanolate in dry THF to give pyridine **8b**, and subsequently oxidized with *m*CPBA to **4b** in an overall yield of 65% (Schemes 5 and 1). The use of AcOOH as the oxidant led to excessive decomposition of pyridine **8b** (presumably due to cleavage of the R−O bond), which was avoided by using *m*CPBA.

2-Chloro-4-propylsulfanylpyridine *N*-oxide (**4e**) was prepared directly from nitro derivative **12** according to a literature procedure described for the benzyl analogue.[19] Thus, treatment of **12** with *n*-PrSH in ethanol in the presence of AcONa gave **4e** as the major product accompanied by small amounts of the 2-propylsulfanyl derivative **14** (Scheme 6).

Experimental Electronic Absorption Spectra. Experimental absorption spectra for the purified esters **1a**−**h** were recorded in MeCN and cyclohexane, and results are shown in Table 1 and Figures 1−3.[20] With the exception of **1e**, all esters exhibit three absorption bands above 200 nm which can be described as $\pi \rightarrow \pi^*$ transitions. The absorption band for the n $\rightarrow \pi^*$ transition, expected above 400 nm, was not observed even for high concentration solutions (10^{-3} M of **1e**).

The observed lowest energy band exhibits significant substituent dependence. For the electron-donating groups, X, the maximum of absorption, λ_{max}, is blue-shifted and for the heptyloxy group the shift is 31 nm in **1b** relative to the parent **1a** (Figure 1). Electron-withdrawing groups, X, decrease the excitation energy, and the λ_{max} for the CN derivative **1f** is red-shifted by 51 nm relative to **1a**. Analysis demonstrated that the observed excitation energies E_{ex} for this absorption band in series **1** generally give poor correlation with substituent constants, which is consistent with previous observations for other series of compounds.[21] The best

(16) Bonnet, V.; Mongin, F.; Trécourt, F.; Quéguiner, G.; Knochel, P. *Tetrahedron* **2002**, *58*, 4429–4438.
(17) Puszko, A.; Talik, Z. *Pol. J. Chem.* **1992**, *66*, 1427–1430. Puszko, A. *Pol. J. Chem.* **1993**, *67*, 837–847.
(18) Talik, Z.; Talik, T. *Rocz. Chem.* **1962**, *36*, 417–422.
(19) Bouillon, C.; Kalopissis, G.; Lang, G. U.S. patent 3,862,305, **1975**.
(20) For details see the Supporting Information.
(21) (a) Shorter J. *Correlation analysis in Organic Chemistry*; Clarendon Press: Oxford, UK, 1973; pp 53−55 and references cited therein. (b) Ford, G. P.; Katritzky, A. R.; Topsom, R. D. In *Correlation Analysis in Chemistry: Recent Advances*; Chapman, N. B., Shorter, J., Eds.; Plenum Press: New York, 1978; pp 298−299.

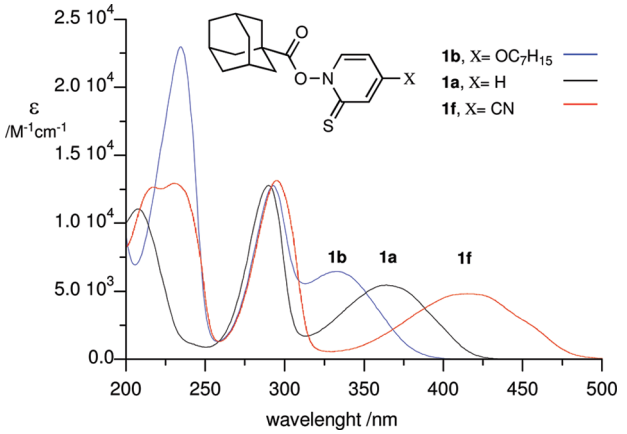

FIGURE 1. Electronic absorption spectra of **1a**, **1b**, and **1f** recorded in MeCN.

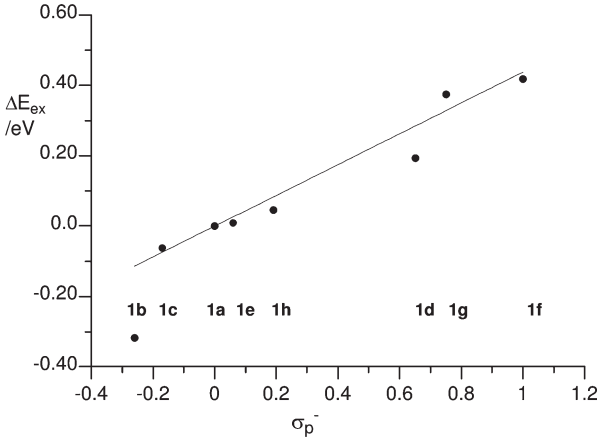

FIGURE 2. Correlation of the relative excitation energy ($\Delta E_{ex} = E_H - E_x$) of **1** in MeCN and the substituent parameter σ_p^-: (excluding **1b**) $\rho = 0.41 \pm 0.03$, $r^2 = 0.95$.

correlation of the relative E_{ex} values (ΔE_{ex}) in MeCN is obtained with the σ_p^- substituent constant,[22] if the data point for **1b** is excluded (Figure 2). Trends in other series of substituent constants such as σ_p, σ_p^+, and σ_R^0 (from ^{19}F NMR)[21] do not parallel those observed for E_{ex} in series **1** in MeCN and the corresponding correlations are of significantly lower quality. Excitation energies obtained for **1** in cyclohexane correlate well with the σ_R^0 parameter,[21] if the data point for **1h** is excluded ($E_{ex} = 3.21 - 1.03\sigma_R^0$ eV, $r^2 = 0.97$).

The middle absorption band for series **1** is located at about 290 nm, and its position is practically independent of the substituent. The only exception is the 4-propylsulfanyl group for which the band in **1e** has an unusually large blue shift of 6 nm relative to the parent **1a** and its intensity is over double relative to other esters in the series.[20] Considering that the high-energy band at about 210 nm is largely absent in **1e**, the observed band at 284 nm apparently is a combination or superposition of the two high-energy bands.

Analysis of the substituent effect on the K-band of enones[24] supports this suggestion. Alkyl and chlorine in the β position exert a small bathochromic shift of +12 nm on the $\pi \rightarrow \pi^*$ transition band of the enone,[24] while for derivatives **1c** and **1h**, enthiones, the shift is +8.5 and +19 nm, respectively, relative to the parent **1a** in MeCN. For the OMe group the effect is +30 nm in enones, while +27 nm is observed in **1b**. The large increment of +85 nm, reported for the SR group in the β position of an enone,[24] predicts the K-band for **1e** at 293 nm, while the unusual peak in this derivative is observed at 284 nm.

A comparison of spectra recorded for **1** in MeCN with those obtained in cyclohexane demonstrates a modest negative solvatochromic effect for the two lowest energy absorption bands (Figure 3). The polar solvent exerts a blue shift ranging from 4 nm for **1f** to 16 nm for **1a** for the lowest energy absorption band, and about 6 nm for the band near 290 nm. The only exception is **1e** for which the complex absorption band at 281.5 nm with visible shoulder features in cyclohexane is red-shifted by 2.5 nm in MeCN. A similar solvatochromic effect was reported for the *N*-trimethylacetoxy

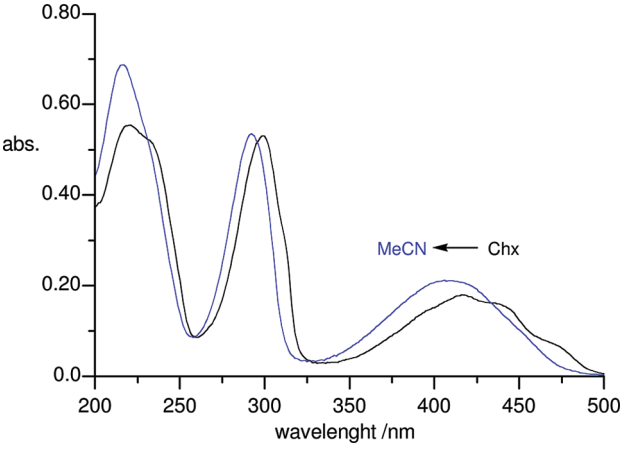

FIGURE 3. Electronic absorption spectra for **1g** in MeCN (blue) and cyclohexane (black).

analogue of **1a**.[25] Spectra of several compounds in cyclohexane exhibit vibronic structures for the lowest energy transition.

Photochemical Stability. The substituent effect on the stability of the Barton esters was assessed by exposing samples of **1a**, **1b**, and **1f** in dry acetone-d_6 to a laboratory standard fluorescent light. NMR analysis demonstrated that after 45 min ~95% of the cyano derivative **1f** was transformed to a major product. During the same time, the parent ester, **1a**, decomposed to the extent of 27%, while the decomposition of the heptyloxy derivative, **1b**, was at a level of about 5%. After another 60 min, all **1f** was completely decomposed, the parent **1a** was transformed by about 55%, and the heptyloxy, **1b**, was decomposed to the extent of 12%. After 16 h all samples were completely decomposed giving a single product (**1b**), two products in 2:1 ratio (**1f**), or an equimolar mixture of two products (**1a**). In ambient daylight the decomposition process is faster. The products of photodecomposition were not isolated, but the major component is assumed to be the expected[23] 4-substituted 2-(adamant-1-ylsulfanyl)pyridine.

(22) Hansch, C.; Leo, A.; Taft, R. W. *Chem. Rev.* **1991**, *91*, 165–195.
(23) Barton, D. H. R.; Crich, D.; Motherwell, W. B. *Tetrahedron* **1985**, *41*, 3901–3924.
(24) Scott, A. I. *Interpretation of Ultraviolet Spectra of Natural Products*; Prergamon Press: New York, 1964; p 58.
(25) Aveline, B. M.; Kochevar, I. E.; Redmond, R. W. *J. Am. Chem. Soc.* **1995**, *117*, 9699–9708.

The observed order of the rate of photodecomposition for the three derivatives (**1f** > **1a** > **1b**) is consistent with the relative intensity of absorption in the visible range (> 400 nm) in the series (see Figure 1).

Computational Analysis. To gain a better understanding of the nature of the electronic excitations and the substituent effect on their energies in series **1**, we conducted TD-DFT and ZINDO calculations for the closely related *N*-acetates **2** at the equilibrium geometries obtained at the B3LYP/6-311G(d,p) level of theory. TD-DFT vertical excitation energies were calculated by using the B3LYP functional in combination with either 6-311G(d,p) or cc-pVDZ basis sets.

Geometry optimizations demonstrated that the *N*-acetoxy group is nearly orthogonal to the pyridine ring as a result of repulsion of electron pairs on the adjacent N and O atoms. This is consistent with the solid-state structure for 1-(4-*tert*-butylcyclohexanecarbonyloxy)pyridine-2(1*H*)-thione[26] and results of our recent calculations for another series of pyridine-2(1*H*)-thione derivatives.[27] Most substituents in the 4 position are coplanar with the pyridine ring (Figure 4). The only exception is the acetoxy group in **2*l***, which forms a dihedral angle (defined by $C_{ring}-C_{ring}-O-C(=O)$) of 32° with the pyridinethione ring. The CH_3 and CF_3 groups in **2c** and **2d** adopt the eclipsed conformation.

Both TD-DFT and ZINDO//DFT calculations of series **2** reproduced the general trends observed in series **1**, including the substituent impact on the energies of the main absorption bands. The results showed that the low-energy electronic absorptions involve two highest occupied and two lowest energy virtual MOs. The DFT results demonstrated that the HOMO orbital is localized on the sulfur atom and contains the lone pair (n_{CS}). The remaining 3 orbitals are of π type MOs and generally involve mainly the thiono group (HOMO-1, π_{CS} and LUMO+1, π^*_{CS}) or the ring (LUMO, π^*_{ring}, Figure 5). The substituents with strong electron-donating or -accepting properties significantly perturb the pyridinethione MO system. Thus, the NMe_2 in **2k** switches order of the n_{CS} and π_{CS}, and the latter becomes the HOMO. Similarly, for the strongly electron-withdrawing NO_2 in **2n** the π^*_{CS} and π^*_{ring} MOs are altered and both have density extending from the ring to the substituent.

Substituents with lone pairs (OMe, SMe, Cl, NMe_2, OAc) and high-lying π electrons (C≡CH) interact with the π system of the pyridinethione ring. Consequently, the resulting π_{ring} orbital has density extending into the substituent and becomes the HOMO-2, as shown for **2i** in Figure 5. In these esters, the HOMO-3 (n_{CO}) and LUMO+2 (π^*_{CO}) are localized on the *N*-acetoxy group (Figure 5).

The two sets of TD-DFT results are similar. The cc-pVDZ basis set computes the $n_{CS} \rightarrow \pi^*_{ring}$ and $\pi_{CS} \rightarrow \pi^*_{ring}$ transitions at slightly lower energy (−0.06 and −0.03 eV, or 9.5 and 3 nm, respectively) and the $\pi_{CS} \rightarrow \pi^*_{CS}$ transition at slightly higher energy (0.08 eV or −5 nm) than those obtained with the 6-311G(d,p) basis set.

The TD-B3LYP/cc-pVDZ//B3LYP/6-311G(d,p) results revealed that the electronic excitations are located in four areas of the spectrum. On the basis of the major transitions, these excitations can be classified as the $n_{CS} \rightarrow \pi^*_{ring}$ (λ > 380 nm, $f \leq 1 \times 10^{-4}$), the $\pi_{CS} \rightarrow \pi^*_{ring}$ (λ = 340 to 475 nm, $f \approx 5 \times 10^{-2}$), the $\pi_{CS} \rightarrow \pi^*_{CS}$ ($\lambda \approx 270$ nm, $f \approx 0.2$), and the $\pi_{ring} \rightarrow \pi^*_{ring}$ (λ < 250 nm). In addition, all esters exhibit CT excitations from the C=S group to the C=O of the *N*-acetoxy, $n_{CS} \rightarrow \pi^*_{CO}$ and $\pi_{CS} \rightarrow \pi^*_{CO}$ ($f \approx 1 \times 10^{-2}$), at about 280 nm. The latter transition combines with the $\pi_{CS} \rightarrow \pi^*_{CS}$ transition, and it constitutes a significant component of this electronic excitation in several esters.

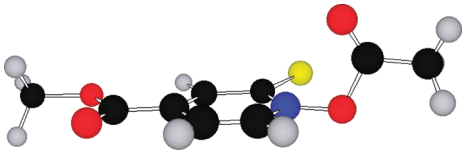

FIGURE 4. B3LYP/6-311G(d,p) optimized geometry of **2g**.

The $n_{CS} \rightarrow \pi^*_{ring}$ transition is very weak and has not been observed experimentally. The computed energies and their substituent dependence for the remaining three main transitions in **2** are in general agreement with the experimental results obtained for **1**. Thus, the computational results reproduced the experimentally observed strong substitent dependence for the $\pi_{CS} \rightarrow \pi^*_{ring}$ transition and weak dependence for the $\pi_{CS} \rightarrow \pi^*_{CS}$ transition. Theoretical results for the former transition correlate well with the experimental data in cyclohexane except for the data points for the derivatives with strongly electron-withdrawing substituents CN and COOMe (**2f** and **2g**). The correlation factor $r^2 = 0.98$ for the cyclohexane data is higher than that for the MeCN data (r^2 = 0.96, Figure 6), presumably due to the solvent effect that is not included in the TD-DFT model.

The calculated $\pi_{ring} \rightarrow \pi^*_{ring}$ excitations are less reliable. They show, however, that certain substituents such as SMe, NMe_2, and C≡CH exhibit strong electronic coupling with the ring, which results in significant decrease of the excitation energy and increase of the oscillator strength. The largest red shift for the $\pi_{ring} \rightarrow \pi^*_{ring}$ excitations is calculated for the SMe derivative (E_{ex} = 259 nm and $f \approx 0.43$), which is consistent with the experimentally observed apparent merger of the $\pi_{ring} \rightarrow \pi^*_{ring}$ and $\pi_{CS} \rightarrow \pi^*_{CS}$ transitions at λ_{max} = 281.5 nm in cyclohexane and at λ_{max} = 284 nm in MeCN for **1e** (Table 1, vide supra).

The ZINDO calculations are generally in agreement with the TD-DFT results. However, the ZINDO calculated energies for the $n_{CS} \rightarrow \pi^*_{ring}$ and $\pi_{CS} \rightarrow \pi^*_{ring}$ excitations have a

TABLE 1. Absorption Maxima for Esters 1 in MeCN

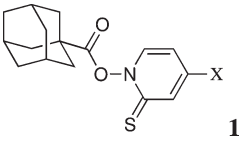

1

1	X	λ_{max} (log ε) (nm)	λ_{max} (log ε) (nm)	λ_{max} (log ε) (nm)
a	H [a]	208 (4.05)	290 (4.11)	364 (3.74)
b	OC_7H_{15}	235 (4.36)	293 (4.11)	333 (3.81)
c	Me	216.5 (4.22)	292.5 (4.15)	357.5 (3.80)
d	CF_3	208 (4.1)	292.5 (4.16)	386 (3.73)
e	SC_3H_7		284 (4.45)	365 (3.75)
f	CN	216 (4.1) and 230 (4.1) [b]	294.5 (4.12)	415 (3.69)
g	COOMe	216(4.20)	292 (4.09)	409 (3.68)
h	Cl	227 (4.22)	295 (4.17)	369 (3.73)

[a]Reference 23: λ_{max} (log ε) 364 (3.64) and 286 (4.15) in EtOH. [b]See Figure 1.

(26) Hartung, J.; Hiller, M.; Schwarz, M.; Svoboda, I.; Fuess, H. *Liebigs Ann.* **1996**, 2091–2097.
(27) Kaszynski, P. *Phosphorus, Sulfur, Silicon Relat. Elem.* **2009**, *184*, 1296–1306.

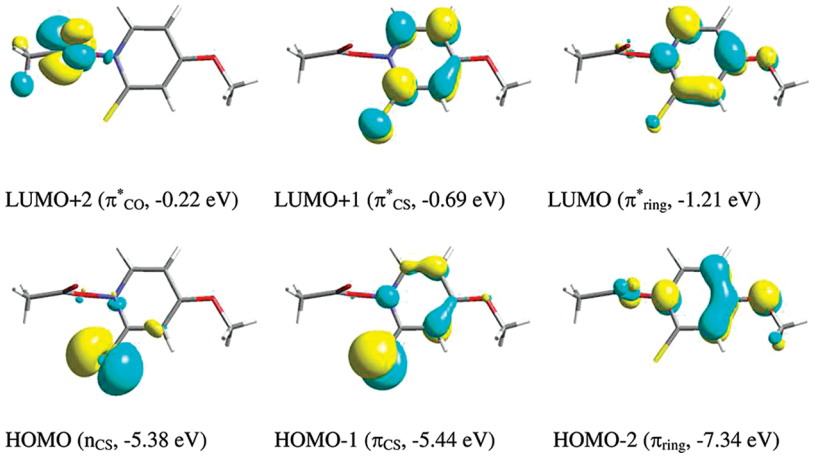

FIGURE 5. B3LYP/cc-pVDZ generated contours of molecular orbitals for **2i** relevant to the low-energy transitions.

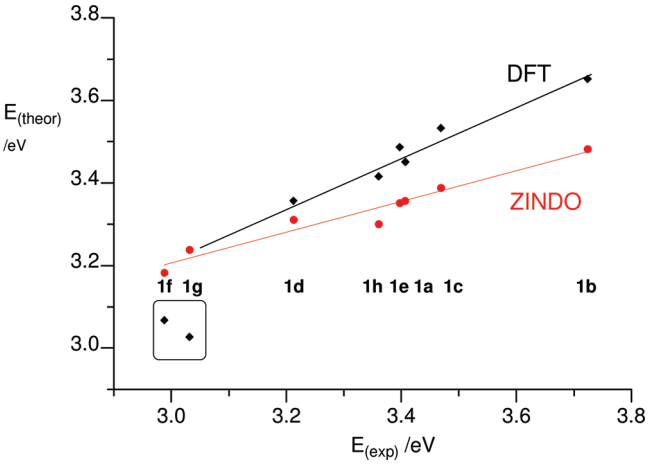

FIGURE 6. Correlation of the experimental (for **1** in MeCN) and theoretical (for **2**) excitation energies. Best fit lines: ZINDO (red circles, all data): $E_{(theor)} = 2.01 + 0.372E_{(exp)}$, $r^2 = 0.95$; TD-B3LYP/cc-pVDZ (black diamonds, excluding **g** and **f**): $E_{(theor)} = 1.55 + 0.553E_{(exp)}$, $r^2 = 0.96$.

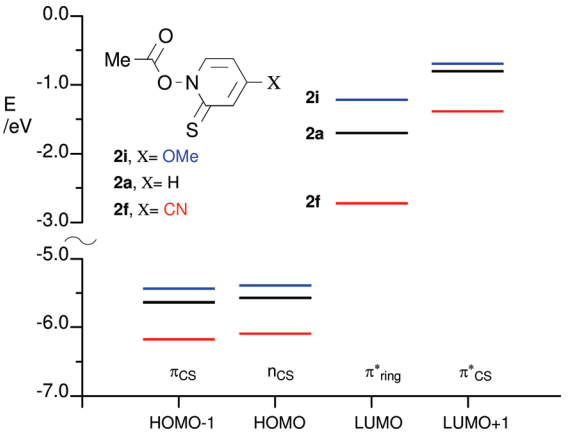

FIGURE 7. Substituent effect on MO energy: B3LYP/cc-pVDZ derived energy levels for **2a** (black), **2f** (red), and **2i** (blue).

more narrow range, the order of n_{CS} and π_{CS} is reversed, and the low-intensity excitations to the *N*-acetoxy π^*_{CO} are absent. On the other hand, the ZINDO results give more realistic values of the oscillator strength, $f \approx 0.2$, for the two observed excitations $\pi_{CS} \rightarrow \pi^*_{ring}$ and $\pi_{CS} \rightarrow \pi^*_{CS}$, and appropriate energy for the latter transition at about 300 nm. In addition, the ZINDO calculated excitation energies correlate relatively well with all the experimental data points (Figure 6). The quality of the correlation for data obtained in MeCN and cyclohexane is practically identical.

Analysis of the ZINDO results for **2** demonstrated that the excitation energies calculated in MeCN dielectric medium are generally blue-shifted by an average of 28 ($n_{CS} \rightarrow \pi^*_{ring}$), 7 ($\pi_{CS} \rightarrow \pi^*_{ring}$), and 8 nm ($\pi_{CS} \rightarrow \pi^*_{CO}$). This is consistent with the experimentally observed negative solvatochromic effect in series **1** and an average blue shift of 9 and 5 nm for the two $\pi \rightarrow \pi^*$ transitions. The only exception is the $\pi_{CS} \rightarrow \pi^*_{ring}$ transition for **2n** (X = NO_2) and the $\pi_{CS} \rightarrow \pi^*_{CS}$ transition for **2k** (X = NMe_2), for which a red shift of 1 and 16 nm, respectively, is calculated in the polar medium.

The origin of the substituent effect on absorption spectra was investigated by using the DFT results for esters **2a**, **2f**, and **2i** in Figure 7. Analysis shows that the OMe substituent destabilizes all four orbitals with the largest effect on the LUMO (+0.49 eV). Conversely, the CN substituent stabilizes all four orbitals, with the largest effect exerted again on the LUMO (−1.02 eV). The remaining three orbitals have lower energies by a similar value of about 0.55 eV relative to **2a**. Thus, transitions involving excitation to the LUMO, which is designated as π^*_{ring}, are expected to exhibit the strongest substitent effect. Indeed, both low-energy transitions, $n_{CS} \rightarrow \pi^*_{ring}$ and $\pi_{CS} \rightarrow \pi^*_{ring}$, involve the LUMO ($\pi^*_{ring}$) and both show strong dependence on the substituent, while the band at about 290 nm involves the HOMO−LUMO+1 transition ($\pi_{CS} \rightarrow \pi^*_{CS}$), which renders it practically substituent independent. Consequently, the observed trends in $n_{CS} \rightarrow \pi^*_{ring}$ and $\pi_{CS} \rightarrow \pi^*_{ring}$ excitation energies follow those of the LUMO energy. Also, the calculated $n_{CS} \rightarrow \pi^*_{ring}$ excitation energies correlate with the σ_p^- parameter as shown in Figure 8.

Discussion and Conclusions

Experimental photophysical studies revealed that the position of the observed lowest energy absorption band is

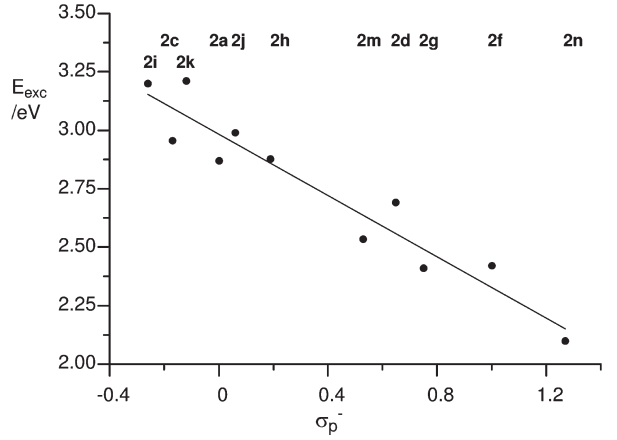

FIGURE 8. Correlation of the excitation energy E_{exc} (B3LYP/cc-pVDZ) for the $n_{CS} \rightarrow \pi^*_{ring}$ transition in **2** and the substituent parameter σ_p^-. $E_{exc} = 2.98 - 0.66\sigma_p^-$, $r^2 = 0.92$.

sensitive to the substituent in the 4-position and varies from 333 nm for RO to 415 nm for CN. As a consequence, the esters have differential sensitivity to light: the cyano derivative **1f** undergoes photoinduced transformation about 20 times faster than the alkoxy derivative **1b** under the same conditions. The position of the higher energy absorption band at about 295 nm is practically substituent independent. Both bands exhibit a modest negative solvatochromic effect.

Analysis of the TD-DFT and ZINDO results revealed the electronic structure and the nature of the observed electronic excitations in series **1**. In general, our results are consistent with those of previous computational studies of nitro and fluoro derivatives of 1-methoxypyridine-2(1*H*)-thione.[12] They demonstrate that the substituent in the 4-position strongly affects the energy level of the LUMO (π^*_{ring}) and consequently the position of the absorption maxima of two lowest energy transitions: the unobserved $n_{CS} \rightarrow \pi^*_{ring}$ and the observed $\pi_{CS} \rightarrow \pi^*_{ring}$. Out of the two transitions, the latter appears to have the dominant effect on the photostability of the ester. The experimentally unobserved $n_{CS} \rightarrow \pi^*_{ring}$ transition has a significantly lower absorption coefficient and is predicted to appear >390 nm for all esters in series **1**, which suggests similar weak sensitivity to visible light for all members of the series. Further analysis of the series **2** revealed that the 4-RO substituent exerts the nearly maximum effect on increasing the excitation energy (largest blue shift) and hence provides the maximum photostabilization for esters in series **1**. A similar position of the absorption maximum and consequently photostability can be expected for the 4-NMe_2 derivative **1k**.

Computational results are moderately useful as a tool for the prediction of excitation energies. The TD-DFT method has a problem with good reproduction of energies for the electron-deficient species such as **1f** and **1g** (Figure 6) and the magnitude of the oscillator strength. In contrast, the ZINDO//DFT method performs better and provides a better correlation with all experimental results, despite a more narrow range of computed excitation energies (the slope of the correlation line is 0.37). The best predictive tool, however, appears to be the Hammett-type correlation shown in Figure 2.

Correlation between the experimental excitation energies and the σ_p^- substituent parameter in Figure 2 permits an estimate of the λ_{max} for unknown derivatives of **1**. Thus, λ_{max} for **1n** (X = NO_2) is predicted at 430 nm in MeCN. A value of 413 nm is predicted for the same derivative **1n** on the basis of ZINDO results and the correlation in Figure 6. However, this value seems too low considering that λ_{max} for **1f** (X = CN) is 415 nm. Derivative **1** with the $MeSO_2$ group ($\sigma_p^- = 1.13$)[22] in the 4 position has a predicted λ_{max} value of 421 nm, and the CF_3SO_2 group ($\sigma_p^- = 1.63$),[22] which is one of the most electron-withdrawing substituent, shifts the $\pi_{CS} \rightarrow \pi^*_{ring}$ absorption to 452 nm, according to Figure 2.

The presented results demonstrate synthetic methods for the preparation of substituted 1-hydroxypyridine-2(1*H*)-thiones, offer basic understanding of the photophysical processes, and provide a predictive tool for designing *N*-acyloxy derivatives with desired light sensitivity.

Computational Details

Quantum-mechanical calculations were carried out with the Gaussian 98 suite of programs.[28] Geometry optimizations were undertaken by using the B3LYP functional[29,30] with the 6-311G(d,p) basis set,[31] default convergence limits, and without symmetry constraints. Vibrational frequencies were used to characterize the nature of the stationary points. Vertical electronic excitation energies for esters **2** were obtained by employing the TD-DFT method[32] and using the B3LYP functional[29,30] with the 6-311G(d,p)[31] or cc-pVDZ[33] basis sets. Excitation energies for **2** were also obtained at their DFT determined geometries by using the INDO/2 algorithm (ZINDO)[34] as supplied in the Cerius2 suite of programs and including all electrons and orbitals in the CI. ZINDO calculations with the solvation model (Self Consistent Reaction Field) used cavity radii derived from the DFT calculations with the VOLUME keyword.

Experimental Section

Melting points are uncorrected. ^{1}H NMR and ^{13}C NMR spectra were recorded at 300 and 75 MHz, respectively, in $CDCl_3$, unless specified otherwise. Chemical shifts were referenced to the solvent ($CHCl_3$ set at 7.26 and 77.0 ppm). UV spectra were recorded in CH_3CN and cyclohexane. Molar

(28) Frisch, M. J.; Trucks, G. W.; Schlegel, H. B.; Scuseria, G. E.; Robb, M. A.; Cheeseman, J. R.; Zakrzewski, V. G.; Montgomery, J. A., Jr.; Stratmann, R. E.; Burant, J. C.; Dapprich, S.; Millam, J. M.; Daniels, A. D.; Kudin, K. N.; Strain, M. C.; Farkas, O.; Tomasi, J.; Barone, V.; Cossi, M.; Cammi, R.; Mennucci, B.; Pomelli, C.; Adamo, C.; Clifford, S.; Ochterski, J.; Petersson, G. A.; Ayala, P. Y.; Cui, Q.; Morokuma, K.; Malick, D. K.; Rabuck, A. D.; Raghavachari, K.; Foresman, J. B.; Cioslowski, J.; Ortiz, J. V.; Baboul, A. G.; Stefanov, B. B.; Liu, G.; Liashenko, A.; Piskorz, P.; Komaromi, I.; Gomperts, R.; Martin, R. L.; Fox, D. J.; Keith, T.; Al-Laham, M. A.; Peng, C. Y.; Nanayakkara, A.; Challacombe, M.; Gill, P. M. W.; Johnson, B.; Chen, W.; Wong, M. W.; Andres, J. L.; Gonzalez, C.; Head-Gordon, M.; Replogle, E. S.; Pople, J. A. *Gaussian 98*, Revision A.9; Gaussian, Inc., Pittsburgh, PA, 1998.
(29) Becke, A. D. *J. Chem. Phys.* **1993**, *98*, 5648–5652.
(30) Lee, C.; Yang, W.; Parr, R. G. *Phys. Rev. B* **1988**, *37*, 785–789.
(31) (a) McLean, A. D.; Chandler, G. S. *J. Chem. Phys.* **1980**, *72*, 5639–5648. (b) Krishnan, R.; Binkley, J. S.; Seeger, R.; Pople, J. A. *J. Chem. Phys.* **1980**, *72*, 650–654.
(32) (a) Bauernschmitt, R.; Ahlrichs, R. *Chem. Phys. Lett.* **1996**, *256*, 454–464. (b) Stratmann, R. E.; Scuseria, G. E.; Frisch, M. J. *J. Chem. Phys.* **1998**, *109*, 8218–8224.
(33) (a) Woon, D. E.; Dunning, T. H. Jr. *J. Chem. Phys.* **1993**, *98*, 1358–1371. (b) Dunning, T. H. Jr. *J. Chem. Phys.* **1989**, *90*, 1007–1023.
(34) Zerner, M. C. In *Reviews of Computational Chemistry*; Lipkowitz, K. B. Boyd, D. B., Eds.; VCH Publishing: New York, 1991; Vol. 2, pp 313−366 and references cited therein.

extinction coefficients were obtained by fitting maximum absorbance against concentration in agreement with Beer's law.

The synthesis, isolation, and handling of **1c**−**h** and all its sulfur-containing intermediates were performed in the presence of red light only!

Adamantane-1-carboxylate Esters 1a−**e: General Procedure.** According to a literature procedure,[13] adamantane-1-carbonyl chloride (1.1 mmol) was added to a suspension of crude sodium salt **3**[**Na**] (prepared from 1.0 mmol of *N*-oxide **4**) in dry MeCN (2 mL) and the reaction mixture was stirred overnight. The solvent was evaporated and the residue was passed trough a silica gel plug with use of CH_2Cl_2 as the eluent. The resulting product was purified by repeated recrystallization from MeCN with a few drops of AcOEt.

1-(Adamantane-1-carbonyloxy)-4-trifluoromethylpyridine-2(1*H*)-thione (1d). Crude product was recrystallized from MeCN to give **1d** in 50% yield as a yellow solid: mp 156−158 °C; ^{1}H NMR ($CDCl_3$) δ 1.78 (br s, 6H), 2.09−2.14 (m, 3H), 2.16 (br s, 6H), 6.66 (dd, J_1 = 7.3 Hz, J_2 = 2.3 Hz, 1H), 7.55 (d, J = 7.2 Hz, 1H), 7.86 (br s, 1H); ^{13}C NMR ($CDCl_3$) δ 27.5, 36.0, 38.5, 41.1, 107.4, 121.9 (q, J = 275 Hz), 134.1 (q, J = 35 Hz), 134.5 (q, J = 4.4 Hz), 139.1, 172.4, 175.4. Anal. Calcd for $C_{17}H_{18}F_3NO_2S$: C, 57.13; H, 5.08; N, 3.92. Found: C, 57.05; H, 4.95; N, 4.02.

Analytical data for other compounds **1** are provided in the Supporting Information.

1-Hydroxypyridine-2(1*H*)-thiones 3b−**e: General Procedure.** Crude 1-hydroxypyridine-2(1*H*)-thione sodium salt **3**[**Na**] was treated with dilute HCl and the product was extracted with CH_2Cl_2. The solvent was evaporated to leave thione **3** as a yellowish viscous oil, with purity >90%, based on NMR analysis.

1-Hydroxy-4-trifluoromethylpyridine-2(1*H*)-thione (3d). ^{1}H NMR ($CDCl_3$) δ 6.89 (dd, J_1 = 7.1 Hz, J_2 = 2.2 Hz, 1H), 7.91 (d, J = 2.0 Hz, 1H), 8.19 (d, J = 7.1 Hz, 1H); HRMS calcd for $C_6H_5F_3NOS$ m/z 196.0044, found m/z 196.0062.

Analytical data for other compounds **3** are provided in the Supporting Information.

2-Chloropyridine *N*-Oxides 4b−**d and 4f: General Procedure.** A solution of appropriate 2-chloropyridine **7** (1.0 mmol) and *m*-chloroperoxybenzoic acid (*m*CPBA, 2.0 mmol) in dry CH_2Cl_2 (2 mL) was stirred at rt for 48 h. A saturated solution of Na_2CO_3 was added, the mixture was stirred for 0.5 h and extracted with CH_2Cl_2, the extracts were dried (Na_2SO_4), and solvent was evaporated. The residue was purified on a silica gel plug (CH_2Cl_2 then acetone) to give *N*-oxide **4** as a colorless oil.

2-Chloro-4-trifluoromethylpyridine *N*-Oxide (4d). Yield 37%; mp 42−44 °C; ^{1}H NMR ($CDCl_3$) δ 7.43 (dd, J_1 = 6.8 Hz, J_2 = 2.1 Hz, 1H), 7.75 (d, J = 2.0 Hz, 1H), 8.40 (d, J = 6.8 Hz, 1H); HRMS calcd for $C_6H_4ClF_3NO$ m/z 197.9934, found m/z 197.9917.

Analytical data for other compounds **4** are provided in the Supporting Information.

Acknowledgment. Financial support for this work was received from the National Science Foundation (DMR-0606317). We thank Mr. Jakub Jakowiecki, a visiting student from the laboratory of Prof. M. Makosza (IchO, Warsaw, Poland), for his help with the preparation of 2-bromoisonicotinic acid **9**[**Br**].

Supporting Information Available: Synthetic details and characterization data for all compounds, details of photostability experiment, tabularized NMR spectra for **1**, **3**, **4**, and **5**, tabularized results of TD-DFT and ZINDO calculations, archive of calculated equilibrium geometries for **2**, and selected ^{1}H and ^{13}C NMR spectra. This material is available free of charge via the Internet at http://pubs.acs.org.